MOLEKUL
eISSN: 2503-0310

Articles
https://doi.org/10.20884/1.jm.2026.21.2.18309

New Method of Crotepoxide Isolation from the Rhizome of *Kaempferia rotunda*

Soerya Dewi Marliyana*, Risna Ramadhani, Muhammad Widyo Wartono, Faqih Abil Mahazein

Chemistry Department, Faculty of Mathematics and Natural Sciences, Sebelas Maret University, Surakarta 57126, Indonesia

*Corresponding author email: msoerya@staff.uns.ac.id

Received November 11, 2025; **Accepted** April 08, 2026; **Available online** July 20, 2026

ABSTRACT. *Kaempferia rotunda*, commonly known as *Kunci Pepet*, is a Southeast Asian plant. Among its various compounds, crotepoxide stands out as the major secondary metabolite found in its rhizome, classified under polyoxygenated cyclohexanes. This compound has demonstrated various bioactivities, including antibacterial, antileishmanial, and antimutagenic effects, and shows significant promise as an antitumor agent. The potential therapeutic applications of crotepoxide, spotlight the importance of *K. rotunda* in traditional medicine and modern pharmacology. Previous studies on the isolation of crotepoxide have often employed lengthy purification processes, resulting in low yields. This study aims to develop a simplified method for isolating crotepoxide from *K. rotunda* rhizomes, thereby enhancing the yield. Successful extraction was achieved through maceration technique using acetone as a solvent, followed by purification through recrystallization without using vacuum liquid chromatography and column chromatography methods, resulting in 70.4% crotepoxide. The identification of the compound was confirmed through FTIR and 1D-NMR (^{1}H-NMR and ^{13}C-NMR) analysis, and the results were compared with the literature.

Keywords: crotepoxide, isolation of rhizome, *Kaempferia rotunda*, new method

INTRODUCTION

Cyclohexane epoxide is a class of compounds that can be found naturally and has attracted great attention from synthetic and natural product chemists because of its unusual structure, stereochemistry, biogenesis, and biological activities. Cyclohexane epoxide is known to have tumor-inhibiting, anti-leukemic, and antibiotic activities (Nighat et al., 2009; Yetişkin et al., 2025). Crotepoxide is a secondary metabolite of cyclohexane epoxide that can be found in nature through the isolation process. This compound has a variety of bioactivities such as antibacterial, antitumor, anticancer, and antileishmanial (Diastuti et al., 2019; Gelaw et al., 2012).

Studies have shown that crotepoxide has antibacterial activity against pathogenic bacteria such as *Enterococcus aerogenes* and *Bacillus cereus* (Diastuti et al., 2019). The antimutagenic activity of crotepoxide has also been studied and stated that crotepoxide has significant antigenotoxic activity in the Vitotox test and has the potential to mitigate the risks arising from the consumption of food and feed contaminated with aflatoxin B1 (Makhuvele et al., 2018). According to a review of studies, crotepoxide showed significant antitumor activity against Lewis lung carcinoma cell lines (Pathak & Kumar, 2019) and Walker intramolecular carcinosarcoma (Nighat et al., 2009). Crotepoxide has been evaluated for its antileishmanial activity against *Leishmania aethiopica* (Gelaw et al., 2012). Crotepoxide is also used as a starting material to synthesize new compounds with certain bioactivities, especially as tumor inhibitors (Nighat et al., 2009).

The potential bioactivity offered by crotepoxide makes it widely isolated from plants, such as *Piper attenuatum* which is widely found in India, China, Africa, Southeast Asia and Northern Australia (Pathak & Kumar, 2019) and *Croton macrostachyus* which can be found in Eastern Africa such as Ethiopia, Eritrea, Kenya, Uganda, Tanzania and Nigeria (Gelaw et al., 2012). In Indonesia itself, crotepoxide can be found in the rhizomes of *Kaempferia* genus. *Kaempferia* is a genus of the ginger family consisting about 60 species of small rhizome plants, some of which are medicinal rhizomes (Yeap et al., 2017). *Kaempferia rotunda* is the species that produces the most crotepoxide compared to other *Kaempferia* species. Uniquely, crotepoxide itself is the major compound of the rhizome of *K. rotunda* (Aryantini et al., 2025). Previous research stated that the ethyl acetate and ethanol extracts of *K. rotunda* contain 33.11 and 42.92% of crotepoxide, respectively (Diastuti et al., 2019). *Kaemferia rotunda* is widely cultivated in Indonesia for medicinal purposes. In Java, this plant is familiarly

called *kunci pepet* or *kunir putih*. The distribution of this plant is from the eastern Himalayas, India, Laos, Vietnam, Thailand and Java (Hashiguchi et al., 2022). In Indonesia, especially on the Java island, *K. rotunda* is widely cultivated and flowers in October to January. This herbaceous plant has small roots and fragrant rhizomes that are widely used as traditional medicine for stomach aches, dysentery, diarrhea, colds, and obesity (Elshamy et al., 2019; Hashiguchi et al., 2022; Hasim et al., 2023).

The isolation of crotepoxide has been reported by several literature have often employed lengthy purification processes, resulting in low yields. As reported by Aryantini et al. (2023) who successfully isolated 182.9 mg of crotepoxide from ethanol extract from a total of 12 kg of *K. rotunda* rhizomes using the maceration and vacuum liquid chromatography methods with ethyl acetate, acetone and methanol solvents. Yeap et al. (2017) successfully isolated 22.8 mg of crotepoxide from chloroform extract and 100 mg from ethyl acetate extract from a total of 500 g of *K. angustifolia* rhizomes using the maceration method purified by gravity column chromatography. Meanwhile, Atun and Arianingrum (2015), successfully isolated 140 mg of crotepoxide from the chloroform fraction of polar extract of *K. rotunda* rhizomes using the maceration and fractionation methods with chloroform solvents and purified by gravity column chromatography.

Diastuti et al. (2019) also reported the isolation of crotepoxide from acetone extract of *K. rotunda* rhizome by partition method, vacuum liquid chromatography with ethyl acetate solvent and gravity column chromatography with n-hexane : chloroform : ethyl acetate (5:5:1) solvent. Lotul et al. (2008). reported the isolation of crotepoxide from methanol extract of *K. rotunda* by multistage partition method followed by column chromatography with chloroform and methanol solvents. Meanwhile, Gelaw et al. (2012) reported the isolation of crotepoxide from *Croton macrostachyus* berries by Soxhlet method with petroleum ether solvent then purified by column chromatography with chloroform : ethyl acetate (50% : 50%) solvent. Based on the research report, the isolation of crotepoxide primarily uses chromatography methods, including vacuum liquid chromatography and gravity column chromatography, which consume large amounts of solvent. The chromatography process takes a long time and yields relatively few results.

The synthesis of crotepoxide has also been reported. However, this organic synthesis process has disadvantages related to the complexity of the synthesis, requiring special conditions, reactivity and stability issues, environmental and safety issues, and cost of raw material (Lorbach et al., 2002; Sartori et al., 2021). Therefore, the present study developed a simplified method for isolating crotepoxide to make it more effective.

EXPERIMENTAL SECTION

Material

FTIR Shimadzu IRPrestige-21 (UNS, Surakarta), NMR 500 MHz Agilent (ITB, Bandung), UV-Vis spectrophotometer 1800 Shimadzu (UNS, Surakarta), melting point apparatus (Maspion), rotary evaporator (inScienPro Xlab EVA-700), and UV_{254} lamp are instruments and equipment used in this research. The materials used are *K. rotunda* rhizome powder (B2T2TOOT, Karanganyar), acetone, ethyl acetate, n-hexane, methanol, chloroform, and dichloromethane which are technical grade. Aluminum plate coated with silica gel 60 PF_{254} (0.25 mm) (Merck), Cerium(IV) Sulphate and H_2SO_4 (Merck) were used as spray reagents.

Isolation

A total of 2 kg of *K. rotunda* dry rhizome powder was macerated with acetone (3 x 3.5 L) at room temperature for three days. The acetone extract was filtered and concentrated using a rotary evaporator (55 °C, 250 mmHg, 100 rpm) to obtain 95.63 g of *K. rotunda* acetone extract consisting of four layers. Each layer was separated. The compound profile of each layer was monitored using TLC and the solid layer was selected for further purification using the recrystallization method. A total of 15.44 g of the solid layer was dissolved in 30 mL of acetone then saturated with the addition of 70 mL of n-hexane, marked by the start of the formation of a precipitate, then cooled overnight. The yellow precipitate formed was separated from the solvent and then washed three times with 10 mL of methanol by ultrasonication until a white precipitate was obtained. The precipitate was then filtered using a Buchner filtration and crystallized by dissolving it in 30 mL of acetone. The solution was covered with perforated aluminum foil and evaporated slowly until colorless needle crystals (3.82 g) were formed.

RESULT AND DISCUSSION

Isolation of Crotepoxide

The extract obtained from *K. rotunda* rhizome (2 kg) was 95.63 g consisting of four layers. The upper layer (**U**) was golden yellow oil with a mass of 12.67 g. The middle layer (**M**) was a brown liquid with a mass of 48.34 g. The lower layer (**L**) was a thick, black liquid with a mass of 19.31 g. The fourth layer which was solid layer (**S**) was a brown crystalline solid with a mass of 20.31 g. The acetone extract of *K. rotunda* rhizomes was shown in Error! Reference source not found.. Each layer was separated then its profile was seen using thin layer chromatography (TLC) with the solvent *n*-hexane: ethyl acetate (**Figure 2**).

The fourth layer (**S**), which was a brown crystalline solid layer, was selected for further purification with

the consideration that it had a large mass and based on its characteristics that it was already in the form of a crystalline solid, it would be easier to purify. Apart from that, the TLC profile (**Figure 2**) in the fourth layer (**S**) also only had a few stain spots, so the compound would be easier to separate from the impurities. The crystal purification used recrystallization with saturation and cooling methods. The solid layer that had been separated can be seen in **Figure 3**.

A total of 15.44 g of solid layer (**S**) was dissolved in acetone and slightly heated. Heating was carried out to increase the solubility of the sample in dissolved substances. Acetone was chosen as the crystallization solvent because it is a semipolar solvent which is able to completely dissolve the solid layer (**S**) and is easy to obtain. Acetone is inert so it will not react with the compound to be separated. Acetone would dissolve all compounds in the extract, including polar and non-polar compounds. *n*-hexane as an anti-solvent was added slowly until the solution was saturated. The purpose of adding *n*-hexane was to saturate the solution so that crystals that were slightly more polar will precipitate when the solution was cooled. *n*-hexane was dissolve non-polar compounds and acetone will dissolve polar compounds. Meanwhile, crystals that had properties between the two would precipitate because the solubility between the solvent and the crystal did not comply with the rule "like dissolves like". The solution saturation process is shown in Error! Reference source not found..

Figure 1. Acetone extract of *K. rotunda* rhizome

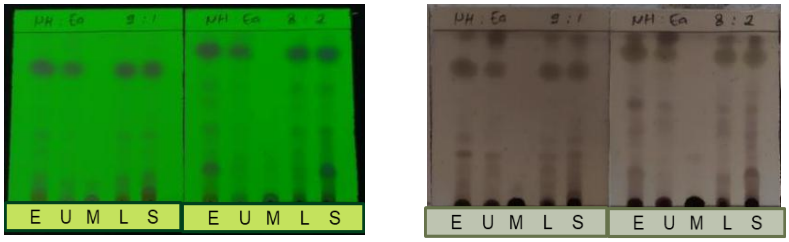

(**a**) (**b**)

Figure 2. TLC profile of each layer of *K. rotunda* extract with *n*-hexane : ethyl acetate eluent, (**a**) seen under UV light λ 254 nm; (**b**) after sprayed with $Ce(SO_4)_2$; E (Extract); U(Upper); M(Middle); L(Lower); L(Liquid); S(Solid)

Figure 3. The solid layer that had been separated from the *K. rotunda* extract

Figure 4. The process of saturating the solution with acetone: n-hexane (1:3).

The saturated solution was cooled so that the compound to be separated could precipitate, while the impurities remain in the saturated solution surrounding the solid (Atun & Arianingrum, 2015). The precipitate formed was separated, resulting in yellow crystalline powder (R1) with a mass of 5.42 g. The recrystallization process in this step was a combination of saturation and cooling recrystallization to obtain maximum yield. The solution was cooled to reduce solubility and accelerate saturation. This cooling method was also done so that the crystals could precipitate completely and could be easily separated from the solution. The crystals obtained were in powder form due to the influence of the cooling rate. The solution was cooled too quickly, resulting in the formation of small crystals in the form of powder (Lorbach et al., 2002). The yellow color of the crystal powder indicated that the crystals were not pure. Compounds that are not pure will not form crystals perfectly. The R1 crystal and its TLC profile can be seen in **Figure 5.**

Based on the TLC profile in **Figure 5**, a faint stain could be seen at the very bottom of the crystal stain. This indicated that the crystal impurity R1 was a polar impurity. The R1 crystal powder was then recrystallized to remove the impurities by washing the crystals with methanol. Methanol was chosen because it is polar so it can dissolve impurities, but not dissolve the crystals. Ultrasonication was carried out so that the lumps of crystal powder could be broken down in order the solvent molecules could reach the impurity particles in the gaps and pores of the crystal. The characteristic of clean crystals was white powder form. The crystals formed were dissolved in acetone and evaporated slowly at room temperature. This aimed to form needle crystals with larger size K9 (crotepoxide). K9 (crotepoxide) can be seen in **Figure 6**.

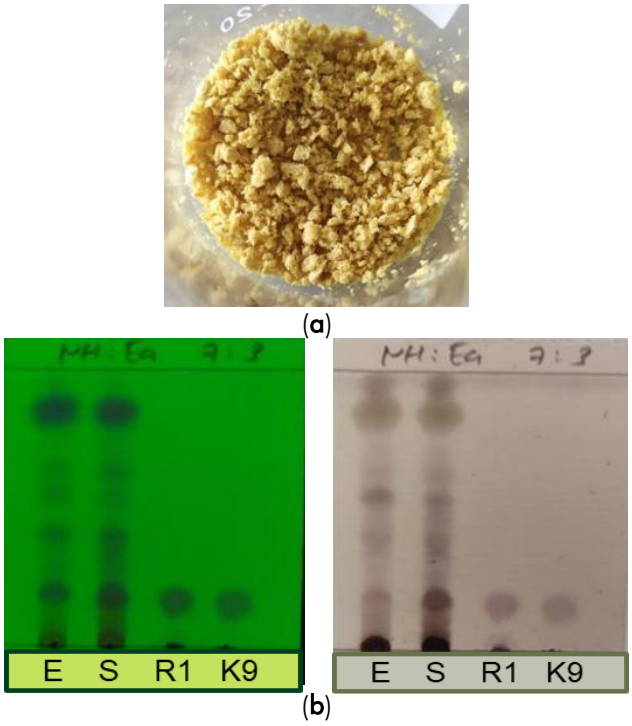

Figure 4. (a) R1 Crystal; (b) TLC profile of extract compared to R1 crystals (*n*-hexane: ethyl acetate 7:3); E(Extract); S(Solid); R1 (yellow crystalline powder); K9 (Crotepoxide).

Figure 5. Pure crystal of K9 isolate (crotepoxide)

The TLC profiles with the eluent *n*-hexane: ethyl acetate (7:3) from K9 and R1 crystals were compared for monitoring. K9 was tested for purity using a three-eluent system, chloroform: ethyl acetate (9:1), chloroform : ethyl acetate : dichloromethane (4:3:1), and n-hexane : chloroform : ethyl acetate (5:5:1) so that a single tailless spot was obtained which indicated that the crystal was pure. Based on the TLC profile in the three-eluent system, it could be seen that each different eluent produced only one spot, so that the crystals obtained were pure. The TLC profile of K9 is shown in **Figure 7**.

Identification of K9 with FTIR

Crotepoxide (K9) that were successfully isolated from the acetone extract of *K. rotunda* rhizomes were identified using FTIR. Identification using FTIR aimed to determine the functional groups contained in the compound. FTIR identification was measured at wave numbers 4000-400 cm^{-1}. The FTIR spectrum can be seen in **Figure 8** and the absorption area can be seen in **Table 1**.

Identification of K9 (crotepoxide) with ^{1}H & ^{13}C NMR

^{13}C-NMR spectroscopy was used to determine the number of carbons and provide an overview of the structural framework. Meanwhile, ^{1}H-NMR was used to determine the number and environment of hydrogen atoms in the compound. The ^{1}H-NMR (500 MHz, $CDCl_3$) and ^{13}C-NMR (125 MHz, $CDCl_3$) analysis spectra of K9 isolate can be seen in **Figure 9** and **Figure 10** and the chemical shifts of both can be seen in **Table 2**.

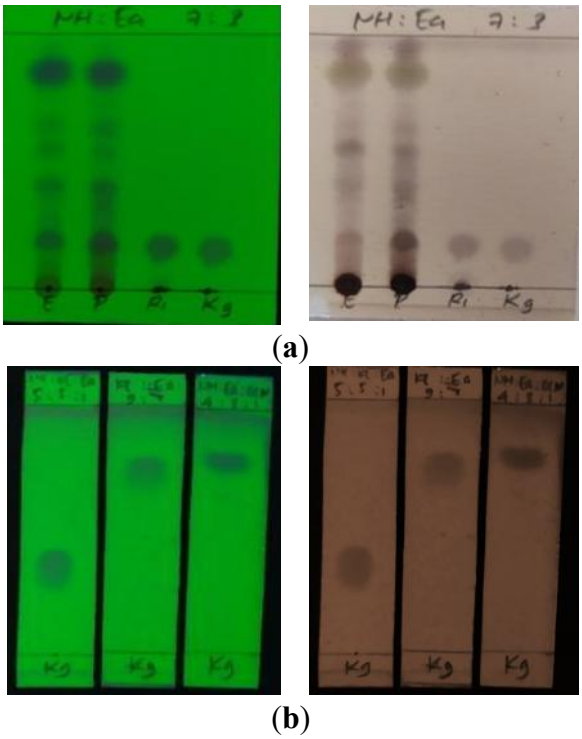

Figure 6. (**a**) Comparison of TLC profiles of extracts and K9; (**b**) K9 purity test with a three-eluents system; E(Extract); S(Solid); R1 (yellow crystalline powder); K9 (Crotepoxide).

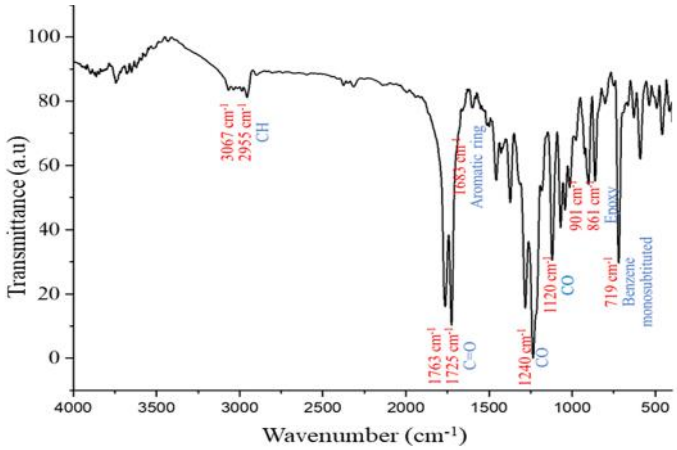

Figure 7 FTIR spectra of isolate K9

Table 1. Absorption areas of functional groups from isolate K9.

Wavenumber (cm^{-1})				Functional Groups
(Yeap et al., 2017)	(Sartori et al., 2021)	(Diastuti et al., 2019)	Isolate K9	
3090			3067	C-H aromatic
2851			2956	C-H methylene
1765	1763	1756	1764	C=O ester acetoxy
1725	1722	1720	1725	C=O ester benzoate
		1686	1683	ArH (Aromatic ring)
1235	1232	1068	1236	C-O epoxy
			1120	C-O ester
903	921		902	Epoxy ring
863	901		862	Epoxy ring
720	718		720	Benzene monosubstituted

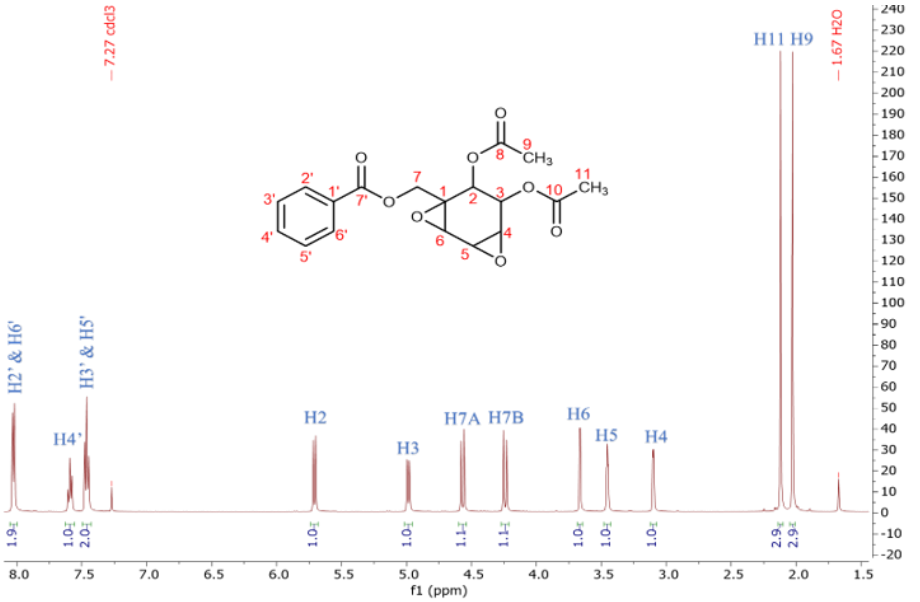

Figure 8. Protons position in the ^{1}H-NMR spectrum of crotepoxide (^{1}H-NMR)

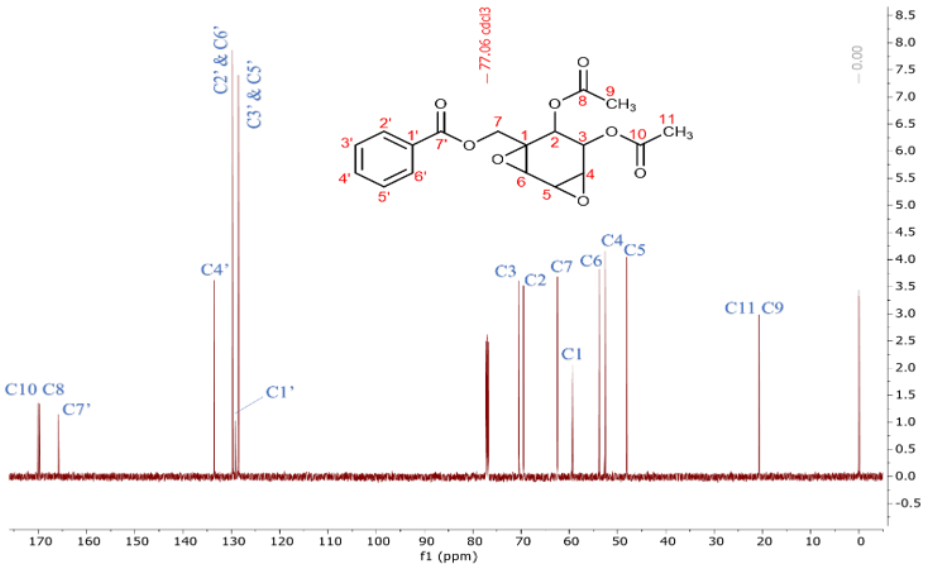

Figure 9. Carbons position in the ^{13}C-NMR spectra of crotepoxide (13C-NMR)

The ^{1}H-NMR spectrum showed the presence of 12 proton signals. Chemical shifts at δ 2.03 and 2.12 ppm showed two singlet peaks, each for the methyl group of the two acetoxy groups at C-9 and C-11 respectively. Peaks at δ 3.10; 3.45; and 3.66 ppm were signals for oxygenated methine protons bound to C-4, C-5, and C-6 respectively on the cyclohexane ring. The AB system peaks at δ 4.57 and 4.24 ppm were methylene proton signals at C-7. The AB system occurred because Ha and Hb were geminal proton couplings (2 bonds distance) in the saturated carbon structure. The AB system in the H7 geminal proton occurred due to limited rotation caused by the influence of steric hindrance from the cyclohexane ring, epoxy ring, benzoyl and acetoxy group, so that the electron density that affected the two hydrogen atoms was different. The peaks at δ 4.99 and 5.71 ppm were proton signals at C-3 and C-2 respectively. Then, peaks at δ 7.46; 7.59, and 8.03 ppm were proton signals on aromatic carbons, respectively for C-3'/C-5', C-4', and C-2'/C-6'.

The ^{13}C-NMR spectra showed the presence of 16 carbon signals. The chemical shifts at δ 20.63 and 20.66 ppm were the carbon signals for C=O in the acetoxy group at C-9 and C-11. The C=O signal on C-11 was located slightly to the left next to the signal on C-9. This was because the carbon on C-11 was more deshielding due to the influence of the benzoyl group attached to the neighboring carbon which increased the electron density on C-11. The chemical shift at δ 62.47 ppm was a signal for methylene carbon from C-7, then the shifts δ 69.47; 70.39; 53.82; 52.62; and 48.07 ppm were the methine carbon signal for C-3, C-2, C-6, C-4, and C-5 respectively. The five carbon signals of methine referred to cyclohexane carbon.

The carbon signal at δ 62.47 ppm referred to the methylene carbon at C-7. Then, peaks at δ 59.42; 129.15; 165.78; 169.74; and 170.04 ppm were signals for quaternary carbon at C-1, C-1', C-7', C-8, and C-10. In addition, there were aromatic carbon signals in the benzene group at δ 128.57; 129.81; and 133.55 ppm for C-3' and C-5', C-2' and C-6', C-4'. There was only one signal for the carbon at C-3' and C-5', C-2' and C-6' for each pair because it was the carbon of a monosubstituted benzene and the structure was symmetrical, so C-3' had the same environment with C-5' producing only one carbon signal at δ 128.57 ppm and C-2' having the same environment as C-6' producing only one signal at δ 129.81 ppm. The carbons at C-2' and C-6' were more deshielding than the carbons at C-3' and C-5' due to the influence of electron resonance in the benzene ring, so the shift was more to the left away from the TMS.

The coupling constant (*J*) value from ^{1}H-NMR was used to determine the dihedral angle of protons in the cyclohexane ring of crotepoxide using the Karplus equation. The Karplus equation explains the mathematical relationship between the visual coupling constant (*J*) in ^{1}H NMR spectroscopy and the dihedral torsion angle (*ϕ*). Because of the limited rotation of the cyclohexane ring, the dihedral angle will affect the *J* value. This is because the structural conformation of the cyclic is more rigid, so that the dihedral angle between neighboring hydrogens remains relatively unchanged and the Karplus equation becomes more relevant. The Karplus equation is shown in equations **1** and **2** (Vaškevičius et al., 2022). The visual coupling of H atoms in the crotepoxide showed in **Figure 11**.

$$J_{Ha\text{-}Hb} = 8{,}5\cos^2\phi - 0{,}28 \quad \text{for } 0° \le \phi \le 90° \qquad \mathbf{1}$$

$$J_{Ha\text{-}Hb} = 9{,}5\cos^2\phi - 0{,}28 \quad \text{for } 90° \le \phi \le 180° \qquad \mathbf{2}$$

Table 2. Comparison of ^{13}C-NMR (125 MHz $CDCl_3$) and ^{1}H-NMR (500 MHz $CDCl_3$) chemical shifts data of crotepoxide with references (Diastuti et al., 2020)

No. C	δ_H (ppm), ΣH, *m*, *J*)*	δ_H (ppm), ΣH, *m*, *J*)	δ_C (ppm)*	δ_C (ppm)
1	-	-	59.39	59.42
2	5.64 (1H, *d*, 9 Hz)	5.71 (1H, *d*, 9.0 Hz)	69.40	69.47
3	4.91 (1H, *d*, 9.2 H	4.99 (1H, *dd*, 9.0 & 1.6 Hz)	70.36	70.39
4	3.03 (1H, *d*, 5 Hz)	3.10 (1H, *dd*, 3.9 & 1.6 Hz)	52.61	52.62
5	3.39 (1H, *dd*, 5 & 2.7 Hz)	3.45 (1H, *dd*, 3.9 & 2.6 Hz)	48.07	48.07
6	3.60 (1H, *d*, 2.7 Hz)	3.66 (1H, *d*, 2.6 Hz)	53.82	53.82
7	4.50 (1H, *d*, 12 Hz) 4.17 (1H, *d*, 12 Hz)	4.57 (1H, *d*, 12.1 Hz) 4.24 (1H, *d*, 12.1 Hz)	62.40	62.47
8	-	-	169.76	169.74
9	1.96 (3H, *s*)	2.03 (3H, *s*)	20.65	20.63
10	-	-	170.06	170.04
11	2.05 (3H, s)	2.12 (3H, *s*)	20.68	20.66
1′	-	-	129.08	129.15
2′ and 6′	7.96 (2H, *dd*)	8.03 (2H, *dd*, 8.4 & 1.5 Hz)	129.79	129.81
3′ and 5′	7.39 (2H, t)	7.46 (2H, *t*, 7.9 Hz)	128.56	128.57
4′	7.53 (1H, *t*)	7.59 (1H, *t*, 7.4 Hz)	133.56	133.55
7′	-	-	165.78	165.78

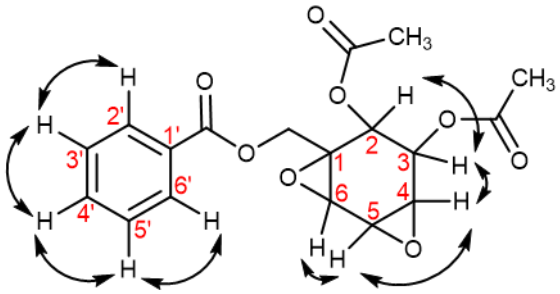

Figure 10. Visual coupling of H atoms in crotepoxide

Table 3. The dihedral angle and position of H in cyclohexane ring of crotepoxide based on calculations using the Karplus equation.

No. H	*m; J(Hz)*	Vicinal Hydrogen Coupling	Dihedral angle (ϕ)	H Position
H_2	*d;* 9.0	H_2-H_3	171.23°	H_2=>Axial
H_3	*dd*; 9.0,	H_3-H_2	171.23°	H_3=>Axial
	1.6	H_3-H_4	61.95°	
H_4	*dd*; 3.9,	H_4-H_5	45.47°	H_4=>Equatorial
	1.6	H_4-H_3	61.95°	
H_5	*dd*; 3.9,	H_5-H_4	45.47°	H_5=>Axial
	2.6	H_5-H_6	54.40°	
H_6	*d*; 2.6	H_6-H_5	54.40°	H_6=>Equatorial

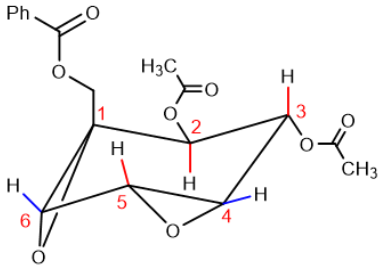

Figure 11. Axial and equatorial positions of the H atom in the cyclohexane ring

Based on the dihedral angle between neighboring hydrogen atoms, the axial-equatorial position of the H in the cyclohexane ring could be determined as shown in **Table 3** and **Figure 12**. This crotepoxide purification method was different from previously reported studies. This research used a simple recrystallization method, while in previous studies, crotepoxide isolation required a fairly long series using the chromatography method. In this research, the solvent used for maceration was acetone, which was different from previous studies because it still used solvents such as ethanol, methanol, chloroform and petroleum ether which had weaknesses compared to acetone. The polarity index of chloroform is 4.4, so it is lower than acetone, so it is less effective for extracting polar compounds. The polarity index of methanol and ethanol is 6.6, so it is higher than acetone, but methanol is generally more toxic, flammable and more dangerous to handle (Quitério et al., 2022). Petroleum ether is nonpolar, with a polarity index of 0.01, so it is less effective for extracting polar compounds.

The crude extract that has been obtained usually contains complex compounds in the form of polar, non-polar and semipolar components, so it needs to be separated based on its polarity with the partition method that had been explained previously. Although the partition method had been successfully applied to separate compounds, the separation stage required a lot of toxic solvents and cannot always be done clearly, and overlapping compounds can be found in successive fractions (Prado & Rostagno, 2013). Previous studies had also used chromatography methods to separate and purify crotepoxide. However, this method took a relatively long time, especially when handling large samples or complex mixtures. The separation requires several processes, plus the drying time and re-operation of the column can increase the overall time required for analysis, requiring a lot of solvent for the elution process (Luxminarayan et al., 2017). In addition, the cost of maintaining a chromatography column is not cheap, is susceptible to contamination from the environment, and can generally only be used for small-scale

separations (Maurya, 2018). Therefore, the purification of crotepoxide was carried out using a simple recrystallization method.

Crotepoxide crystals that were successfully purified by recrystallization were tested for their melting point and gives a melting point of 152-153 °C. According to Diastuti et al. (2020) the melting point of crotepoxide is 152-154 °C , while according to Gelaw et al (2012) the melting point of crotepoxide crystals is 149-150 °C. The yield of crotepoxide crystal by crystallization method (3.82 g from 2 kg) was much higher than the yield that had been reported using chromatography methods, 182.9 mg crotepoxide crystal from 12 kg samples (Aryantini et al. (2023) and 22.8 mg crotepoxide crystal from 500 g samples (Yeap et al. 2017).

CONCLUSIONS

White needle crystals of crotepoxide were successfully isolated from *K. rotunda* rhizomes using the maceration and recrystallization with saturation and cooling methods with a mass of 3.82 g and a yield of 70.4% from the solid layer. This isolation method is simpler, faster, and produces higher yields compared to previously reported methods.

ACKNOWLEDGEMENTS

This research was supported by Sebelas Maret University by Hibah Group Riset No: 371/UN27.22/ PT.01.03/2025

CONFLICT OF INTEREST

There is no conflict of interest in this paper

REFERENCES

Aryantini, D., Astuti, P., Yuniarti, N., & Wahyuono, S. (2023). Bioassay-guided isolation of the antioxidant constituent from *Kaempferia rotunda* L. *Biodiversitas Journal of Biological Diversity*, *24*(6). https://doi.org/10.13057/biodiv/d240665

Aryantini, D., Astuti, P., Yuniarti, N., & Wahyuono, S. (2025). Crotepoxide from *Kaempferia rotunda* L. Inhibit Pancreatic lipase In vitro. *Research Journal of Pharmacy and Technology*, 857–862. https://doi.org/10.52711/0974-360x.2025.00126

Atun, S., & Arianingrum, R. (2015). Anticancer activity of bioactive compounds from *Kaempferia rotunda* rhizome against human breast cancer. *International Journal of Pharmacognosy and Phytochemical Research*, *7*(2), 262–269.

Diastuti, H., Chasani, M., & Suwandri, S. (2020). Antibacterial activity of benzyl benzoate and crotepoxide from *Kaempferia rotunda* L. Rhizome. *Indonesian Journal of Chemistry*, *20*(1), 9. https://doi.org/10.22146/ijc.37526

D.N. Lotul, P., . M., Kardono, L. B. S., & Kawanishi, K. (2008). Antioxidant compound from the rhizomes of *Kaempferia rotunda* L. *Pakistan Journal of Biological Sciences*, *11*(20), 2447–2450. https://doi.org/10.3923/pjbs.2008.2447.2450

Elshamy, A. I., Mohamed, T. A., Essa, A. F., Abd-El Gawad, A. M., Alqahtani, A. S., Shahat, A. A., Yoneyama, T., Farrag, A. R. H., Noji, M., El-Seedi, H. R., Umeyama, A., Paré, P. W., & Hegazy, M.-E. F. (2019). Recent advances in *Kaempferia* phytochemistry and biological activity: A comprehensive review. *Nutrients*, *11*(10), 2396. https://doi.org/10.3390/nu11102396

Gelaw, H., Adane, L., Tariku, Y., & Hailu, A. (2012). Isolation of crotepoxide from berries of *Croton macrostachyus* and evaluation of its anti-leishmanial activity. *Journal of Pharmacognosy and Phytochemistry*, *1*(4), 15–24.

Hashiguchi, A., San Thawtar, M., Duangsodsri, T., Kusano, M., & Watanabe, K. N. (2022). Biofunctional properties and plant physiology of *Kaempferia* spp.: Status and trends. *Journal of Functional Foods*, *92*, 105029. https://doi.org/10.1016/j.jff.2022.105029

Hasim, Faridah, D. N., Afandi, F. A., & Qomaliyah, E. N. (2023). Evaluation of Indonesian anti-obesity traditional plants: A systematic review and meta-analysis on pancreatic lipase inhibition activity. *Food Research*, *7*(6), 145–159. https://doi.org/10.26656/fr.2017.7(6). 892

Lorbach, V., Franke, D., Nieger, M., & MÃ¼ller, M. (2002). Cyclohexadiene-trans-diols as versatile starting material in natural product synthesis: Short and efficient synthesis of iso-crotepoxide and ent-senepoxide. *Chemical Communications*, *5*, 494–495. https://doi.org/10.1039/b110420a

Luxminarayan, L., Neha, S., Amit, V., & M.P. Khinci. (2017). A Review on chromatography techniques. *Asian Journal of Pharmaceutical Research and Development*, *5*(2), 1–8. https://doi.org/10.22270/ajprd.ajprd.com

Makhuvele, R., Foubert, K., Apers, S., Pieters, L., Verschaeve, L., & Elgorashi, E. (2018). Antimutagenic constituents from *Monanthotaxis caffra* (Sond.) Verdc. *Journal of Pharmacy and Pharmacology*, *70*(7), 976–984. https://doi.org/10.1111/jphp.12918

Maurya, A. (2018). Vacuum liquid chromatography: simple, efficient and versatile separation technique for natural products. *Organic & Medicinal Chemistry International Journal*, *7*(2). https://doi.org/10.19080/omcij.2018.07.555710

Nighat, N., Koul, S., Qurishi, M. A., Taneja, S. C., & Qazi, G. N. (2009). Lipase catalyzed regioselective hydrolysis of crotepoxide isolated from *Piper cubeb* Cass DC. *Journal of Molecular Catalysis B: Enzymatic*, *59*(1–3),

121–125. https://doi.org/10.1016/j.molcatb.2009.01.012

Pathak, N., & Kumar, R. (2019). Piper attenuatum Buch.-Ham. Ex Miq. - A review on its macroscopic characters, phytochemistry, medicinal importance and its comparative study with other *Piper* species. *Current Medical and Drug Research*, *3*(02). https://doi.org/10.53517/cmdr.2581-5008.322019198

Prado, J., & Rostagno, M. (2013). *Natural product extraction: Principles and applications*. Royal Society of Chemistry.

Quitério, E., Grosso, C., Ferraz, R., Delerue-Matos, C., & Soares, C. (2022). A critical comparison of the advanced extraction techniques applied to obtain health-promoting compounds from seaweeds. *Marine Drugs*, *20*(11), 677. https://doi.org/10.3390/md20110677

Sartori, S. K., Miranda, I. L., Diaz, M. A. N., & Diaz-Muñoz, G. (2021). Sharpless asymmetric epoxidation: applications in the synthesis of bioactive natural products. *Mini-Reviews in Organic Chemistry*, *18*(5), 606–620. https://doi.org/10.2174/1570193x17999200807141622

Vaškevičius, M., Kapočiūtė-Dzikienė, J., & Šlepikas, L. (2022). Modeling of the crystallization conditions for organic synthesis product purification using deep learning. *Electronics*, *11*(9), 1360. https://doi.org/10.3390/electronics11091360

Yeap, Y. S. Y., Kassim, N. K., Ng, R. C., Ee, G. C. L., Saiful Yazan, L., & Musa, K. H. (2017). Antioxidant properties of ginger (*Kaempferia angustifolia* Rosc.) and its chemical markers. *International Journal of Food Properties*, *20*(sup1), 1158–1172. https://doi.org/10.1080/10942912.2017.1286508

Yetişkin, E., Gündoğdu, Ö., Mete, D., Kishali, N. H., Kara, Y., & Şanlı-Mohamed, G. (2025). Assessment of cytotoxic potentials of isoindole-derived compounds with epoxy alcohol functionalities on different cancer cell lines and molecular docking analysis. *Russian Journal of Bioorganic Chemistry*, *51*(3), 1346–1364. https://doi.org/10.1134/s1068162024606657